J. Nanoanalysis., 5(2): 121-129 Spring 2018

ORIGINAL RESEARCH PAPER

The effect of different pHs, Surfactants and dialyses times on preparation of nano Rod Hydroxyapatite

Fatemeh Mirjalili

Department of Material Engineering, Maybod Branch, Islamic Azad University, Maybod, Iran

Received: 2017-08-12 Accepted: 2018-04-01 Published: 2018-06-30

ABSTRACT

Nano HA rod was synthesized by precipitation method using $Ca(NO_3)_2 4H_2O$ and $(NH_4)_2HPO_4$ as starting materials and ammonia solution as an agent for pH adjustment. The Ca/P molar ratio was maintained at 1.67. Then, the effect of different pH (4, 6, 8, 10, 11), different surfactants and different times for dialyses on nano HA rod were studied in this study. The samples were characterized by different techniques such as, X-ray diffraction, Fourier transform infrared spectra, and Transmission electron microscopies. The XRD analysis showed that the prepared HA nano rod is fully crystalline. The results showed that the best pH for nano HA rod was 11 and Span 20 as the surfactant had the better effect on dispersion and shape of nano rod. The HA nano-rods had an average diameter of 10 nm and length of 70-80 nm after 12 h of dialyses time.

Keywords: *Nano HA Rod, Precipitation Method, XRD Analysis*

How to cite this article

Mirjalili F. The effect of different pHs, Surfactants and dialyses times on preparation of nano Rod Hydroxyapatite. J. Nanoanalysis., 2018; 5(2): 121-129. DOI: 10.22034/jna.2018.542299.1023

INTRODUCTION

Hydroxyapatite is calcium phosphate nearest to bone mineral and the most thermodynamically stable phase in the body [1-3]. Calcium phosphates, including hydroxyapatite for their biocompatibility and similarity to the mineral constituents of bones and teeth are good alternatives for damaged parts of the body [4-6]. Hydroxyapatite raises the capability of bone growth and forms a strong chemical bond with bone tissue when the bone tissue grows in the surface layer of this ceramic [7,8].Nonetheless, it is a brittle material which leads to low mechanical failure and bounds its application in a position under the load.

Materials with nano scale features lead to an improved cellular response, hence they provide the current interest in all micro and nanotechnologies in biomedicine, principally in tissue engineering [9-11]. The fibrous form of HA is particularly promising to be used as a variety of implantable materials; for example, directly as porous bone blocks and defect fillers or through formulation with degradable polymers in order to support cell functions and stimulate regeneration of new tissues [2,12,13].

The techniques used for preparing nano HA rod include chemical precipitation, hydrothermal treatment, sol–gel, micro emulsion techniques, precipitation from complex solutions followed by microwave heating, wet chemical methods, mechanic chemical synthesis and electro deposition [13-20]. Bioactivity of Ca–P based materials is dependent on many factors such as the synthesis procedure, precursor reagents, impurity contents, crystal size and morphology, concentration and mixture order of reagents, pH and temperature [21-25]. Selection of the route of synthesis depends on the application. The present study reports a low temperature synthesis of hydroxyapatite nano rods by a modified and simple precipitation technique.

* Corresponding Author Email: *fm.mirjalili@gmail.com*

Therefore, the novelty of the study is the effect of different PHs on preparation of HA nano rods and modify HA nano rods with different surfactants and then prepare HA nano rods via contorting different dialyses times.

MATERIALS AND METHODS

Nano crystalline hydroxyapatite rod was prepared by a solution-precipitation method via the reaction of calcium nitrate tetra-hydrate ($Ca(NO_3)_2.4H_2O$, 98%, Merck prolabo 0308821 142) with diammonium hydrogen phosphate ($(NH_4)_2HPO_4$, 99%, Merck prolabo A0143307 037) with the molar ratio of Ca/P=1.67. A suspension of 1 M $Ca(NO_3)_2.4H_2O$ was vigorously stirred at 25°C with pH of 10.5-11. After that, 0.67 M $(NH_4)_2HPO_4$ solution was slowly added drop wise to the solution; and the resulting solution was stirred for 1 h and aged for 12 h. Following the separation of the deposition of the reaction solution, the solution was washed with distilled water and dried in an air oven at 100 °C for 2 days to obtain a white powder.

In the next step, after preparing of the solution, different pHs (4, 6, 8 and 10, 11) were adjusted to obtain the most percentage of HA phases. The suspensions of 1 M $Ca(NO_3)_2.4H_2O$ were vigorously stirred at 25°C with different pH. Then, 0.67 M $(NH_4)_2HPO_4$ solution was slowly added drop wise to the solutions and the resulting solutions were stirred for 1 h, aged for 12 h and dried in an air oven at 100 °C for 2 days as previously reported.

In the next step, different surfactants such as span 20 and Aliquid were added to improve the properties. After preparing the first solution of 1 M $Ca(NO_3)_2\ 4H_2O$, the desired surfactants with weight percent of 2.wt% were added and then the second solution of 0.67 M $(NH_4)_2HPO_4$ was slowly added drop wise to the first solution. The resulting solutions were stirred for 1 h, aged for 12 h, washed with distilled water and dried at 100 °C for 2 days.

At last, for improving the properties, different times of dialyses (12, 15, 18 h) were used to provide the best condition for preparing the nano rods. At this stage, after providing the sol, it was dialyzed (dialysis bags-110, B'genei) against deionized water for different times, changing the water every 3 h. The gel obtained after dialysis was dried in an air oven at 100 °C for 2 days to obtain a white powder.

Phase identification was performed by X-ray diffraction (XRD, PW1800, Philips) using nickel filtered Cu Kα radiation in the range of 2θ = 10°-60° with a scanning speed of 5° min^{-1}. Fourier transform infrared spectroscopy (FTIR, Perkin Elmer Spectrum 100) was carried out by the universal attenuated total reflection (UATR) method. Microstructures and morphology of powders were identified by transmission electron microscopy (Philips-Zeiss).

RESULTS AND DISCUSSION

Synthesis of Hydroxyapatite nano rode

This study successfully provided HA nano rod by participation method. The reactions complicated in the formation of HA during the participation preparation and drying could be expressed as follows:

$$10Ca(NO_3)_2 \cdot 4H_2O + 6(NH_4)_2HPO_4\ 20NH_4OH \rightarrow Ca_{10}(PO_4)_6(OH)_2 + 20NH_4NO_3 + 52H_2O \quad (1)$$

The formation of $20NH_4NO_3$ (ammonium nitrate) by product was removed by repetitive washing with twice distilled water (15,16,26).

Fig. 1 shows the XRD peaks of hydroxyapatite rod after drying at 100 for 1 h. The XRD pattern in the figure indicated that the samples were mostly HA phase. On the other side, another crystalline phase (Tricalcium phosphate phase (TCP)) was found in

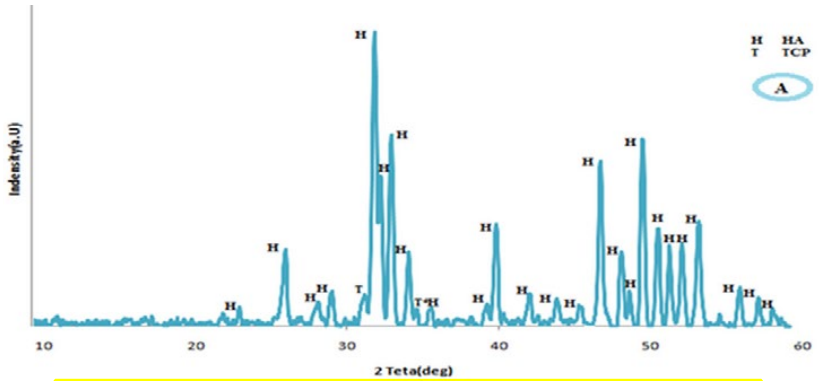

Fig. 1: XRD pattern of pure hydroxyapatite rod synthesized after drying at 100 ° C

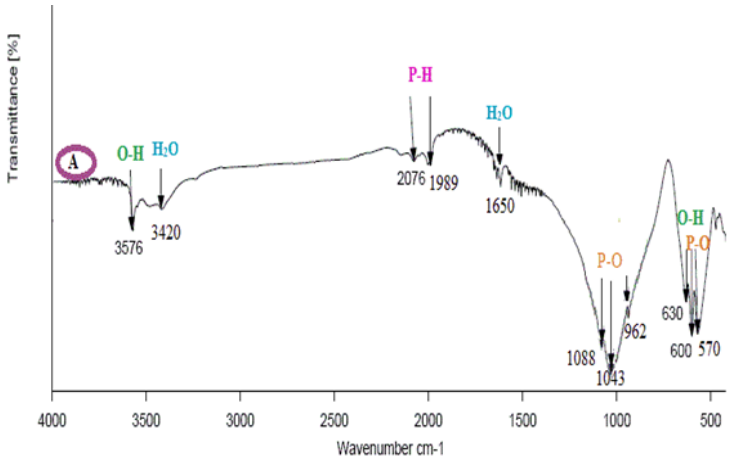

Fig. 2: FTIR curves of pure hydroxyapatite synthesized after drying at 100 ° C

the samples. These results were in close proximity with preparation of HA/Al_2O_3 nanocomposite that were previously reported in the literature (17). The reactions involved in the formation of β-TCP during the chemical precipitation could be expressed as follows:

$$(Ca_{10}(PO_4)_6(OH)_2 \rightarrow 3Ca_3(PO_4)_2 + CaO + H_2O) \quad [11, 12,17] \qquad (2)$$

The size of the crystalline was determined by the Scherrer method.

The equation was calculated as below:

$$t = 0.89\,\lambda / \beta \cos\theta \qquad (3)$$

where, t is grain size, λ is the wave length, β is peak width chosen at half height in radians and θ is the angle in degrees [15].

Equation 2 shows the calculation of crystallinity degree of hydroxyapatite phase by x-ray diffraction patterns of X:

$$Xc = 1-(V_{112/300}-I_{300}) \qquad (4)$$

where Xc is the degree of crystallinity of the powder and $V_{112\,/\,300}$ is the intensity of the cavity between the diffraction peaks (112) and I_{300} [16, 17].

Accordingly, the degree of crystalline of pure hydroxyapatite was about 40% with the crystalline size about 20 nm.

Fig. 2 depicts FTIR analysis of pure HA. The FTIR shows the existence of phosphate (PO_4^{3-}) bonds at 570, 600, 950, and 1100-1090 cm^{-1}, hydroxyl (OH) bonds at 630 and 3567 $cm^{-1}$and P-H band at 1989 and 2076 cm^{-1} that was also reported by previous researchers [8,17,18,27].

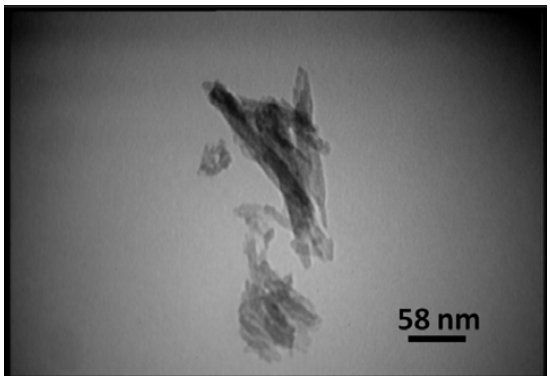

Fig. 3: TEM micrograph of the HA nano rod

Fig. 3 illustrates the TEM morphology of nano HA short rods. It was seen that separate rod-like HA crystals of uniform size and morphology had diameter between 20 to 22 nm and length between 100 and 105 nm. This is in agreement with Kunjalukkal Padmanabha's result which prepared nano rod with 70–90 nm diameter and 400–500 nm length by using a simple sol–gel route and found the possible nanorod nucleation and growth could be related to the relative specific surface energies that connected with the different planes of HA crystal or nucleus (15). The short rods were slightly agglomeration as the size was too small to interweave into a network. This agglomeration between particles is attributed to the large surface area and energy associated with nanoparticles which is compatible to the findings reported by other researchers (15, 16, 28).

Fig. 3 illustrates the TEM morphology of nano HA short rods. It was seen that separate rod-like HA crystals of uniform size and morphology had diameter between 20 to 22 nm and length between 100 and 105 nm as shown in Fig. 3. This is agreement with Kunjalukkal Padmanabhan result which prepared nano rod with 70–90 nm diameter and 400–500 nm length by using a simple sol–gel route and found the possible nanorod nucleation and growth could be related to the relative specific surface energies that connected with the different planes of HA crystal or nucleus (15). The short rods were slightly agglomeration as the size was too small to interweave into a network. This agglomeration between particles is attributed to the large surface area and energy associated with nanoparticles which is in according to other researchers (15,16,28).

The effect of p H on Hydroxyapatite nano rods

Fig. 4 shows the XRD pattern of HA rods at pH=4 (H_1), HA rod at pH=6(H_2), HA rod at pH=8(H_3), HA rod at pH=10(H_4) and HA rod at pH=11(H_5) after drying at 100 °C temperature for 1 h. A comparison diffraction pattern of different pH indicated that formation of a HA phase was the dominant phase in pH=10-11, but the calcium hydrogen phosphate phase was appeared (pH=8) **when** the pH decreased**.** Moreover, at pH=4 and pH=6, the main phase was calcium hydrogen phosphate and some mirror HA phase. A comparison diffraction pattern indicated that decomposition of HA to calcium hydrogen phosphate phase increased by decreasing pH, and the intensity peaks of hydroxyapatite phase decreased and according to Z. Evis, it was responsible for increasing the degradation rate of hydroxyapatite phase (20). When lower pH increased, the reaction between CaO derived from hydroxyapatite analysis and phosphate phase and formation of calcium hydrogen phosphate phase was increased and caused the degradation rate of hydroxyapatite phase which was also demonstrated by the previous researchers that examined the effect of pH on nano HA particles and found the best pH for HA phase is 11 (17, 29).

The FTIR curves (Fig. 5) show the existence of phosphate ($PO4^{3-}$) bonds at 570, 600, 950, and 1100-1090 cm^{-1} and hydroxyl (OH) bonds at 630 and 3567 cm^{-1} and the existence of phosphate (P_2O_7) bonds at 800,850 cm^{-1}[2,9,19,20,30]. However, with increasing the pH to 10 and 11, the intensity of phosphate of ($PO4^{3-}$) bonds at 570, 600, 950, and 1100-1090 cm^{-1} was increased which identified the highest percentages of HA phase at these PHs. This result was mainly reported by Tayyebi who found that more calcium aluminate phases were formed in the crystal lattice of HA/Al_2O_3 nanocomposite (17) when deposition of alumina increased at lower pH. Taken together, the results showed that the obtained material after sintering was mostly crystalline HA.

With regard to Figsures 4 and 5, the best pH for

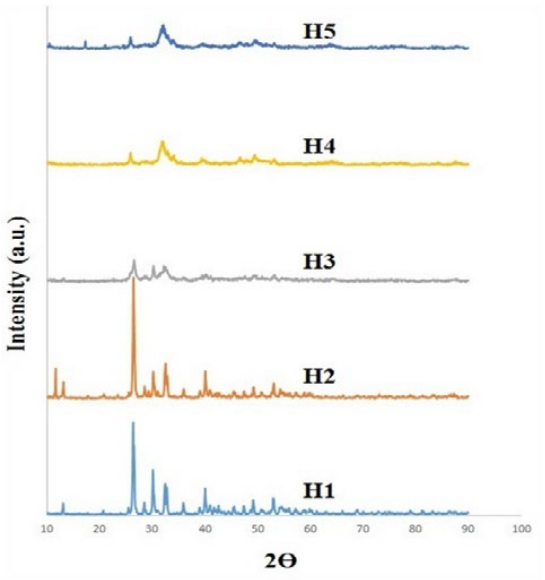

Fig. 4: XRD pattern of HA rod at different PH after drying at 100 °C

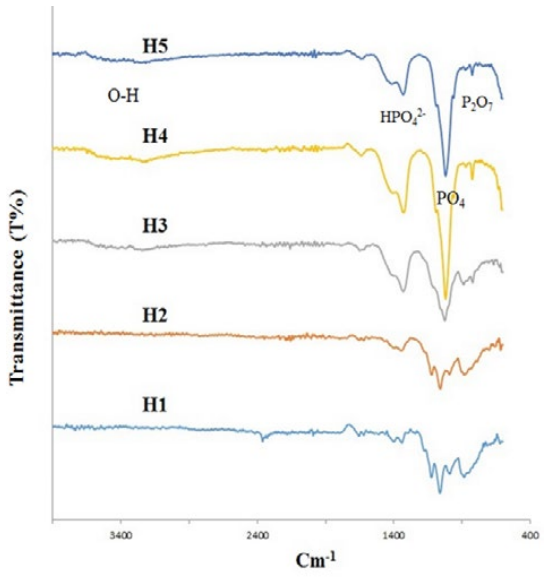

Fig. 5: FTIR curves of HA rod at different PH after drying at 100 °C

preparing nano HA rod was 10- 11 that had the most HA phase comparison with other phosphate phase. This result was also seen in TEM result (Fig. 7) which shows the rods had the finest diameters about 15-20 nm and 100-110 nm length with good dispersion.

As mentioned earlier, the probable nano rod nucleation and growth could be credited to the relative specific surface energies related to the different planes of HA crystal or nucleus, which had unlike surface energies and the planes could define the amount of OH− absorbance from the solution [1,5,7,21-23,30]. In our case, since the solution prepared was preserved at a high pH= 11, different planes would have different OH^- concentration, which would control the growth rate and morphology of the crystal. The surface with high energy would display the increased OH^- concentration, and this perhaps restricted the movement of Ca^{2}+ and $PO4^{3}$− in the formed nucleus in one particular direction. In this situation, OH^- patterned the nucleation process where free Ca^{2}+ and PO_4^{3}− responded with OH in uniaxial direction (planes with less OH− concentration), nucleating into HA nano rods were in agreement with other published data [5]. Fig. 6 represents the situation schematically.

Fig. 7 shows the TEM image of nano HA rod at pH of 11. Certain agglomeration of rods was observed which was related to the large surface area and energy associated with nano rods. The average length of the HA rod seemed to be varied between 120 and 150nm, while the average diameter was found to be between 20 and 25 nm.

Fig. 8 shows the XRD patterns of HA nano rods with different surfactants. According to Fig. 8, dominant phase in both patterns was HA and there was no difference between the patterns. The average crystallite size obtained for the nano rods, using Scherrer's equation, was 15 nm for the span 20 and 25 nm for the Aliquad samples which is in agreement with previous studies. Triethanolamine [11] and TEA [23] were used as capping agents for synthesis of nano particles. In addition, various primary, secondary and tertiary amines were suggested to have shape controlling properties in synthesis of nano particles [22]. Gold nanowires

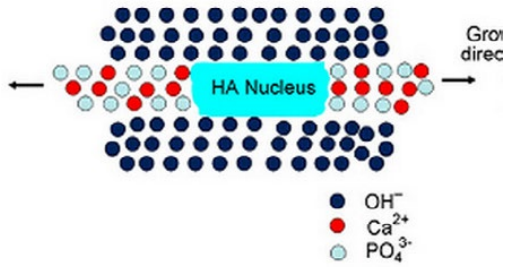

Fig. 6: Schematic representation of nucleation of HA crystals [5]

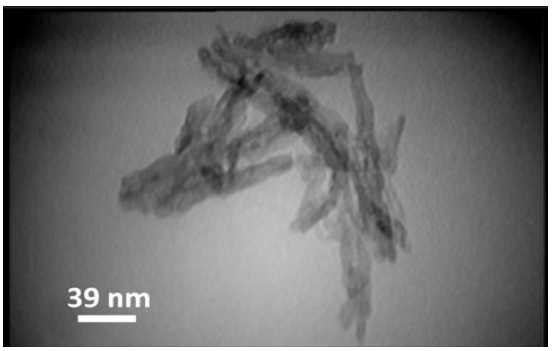

Fig. 7: TEM micrograph of the HA nano rod at pH of 11

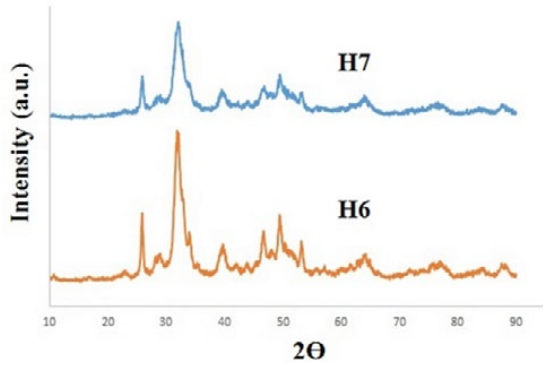

Fig. 8: The XRD pattern of HA rod with Aliquad as a surfactant (H_6) and Span 20 as a surfactant (H_7) after drying at 100 ℃

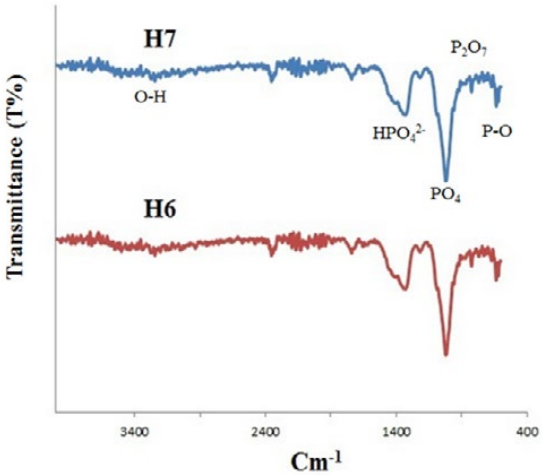

Fig. 9: FTIR curves of HA nano rod with Aliquad as a surfactant (H_6) and Span 20 as a surfactant (H_7) after drying at 100 ℃

were developed from $HAuCl_4$ and TEA where TEA acted as a precursor for the formation of the gold threads [24,30]. It is thought that Rod like nano HA powder is the most favorable building block to construct dental materials [14, 31]. It was shown that dense bioceramics with high strength and fracture toughness could be prepared using 1D HA nanostructures such as nano rods, nanowires, and nano fibers [24,32].

Fig. 9 shows the FTIR curves of HA rod with different surfactants

According to the Fig. 9, there is no difference between the patterns. The characteristic signature HA peak near 600 cm^{-1} was related to the bending modes of P–O bonds in phosphate groups with contribution from the –OH of the apatite group at about 630 cm^{-1} [1, 12, 23, 30]. The small peaks in the region 3300 cm^{-1} were attributed to –OH bonds and those observed near 3472 cm^{-1} were associated to OH^{-1} stretching vibration of HA [6]. The peaks noted around 1100–1000 cm^{-1} were recognized to the stretching modes of the $PO4^{3-}$bonds in HA [7,24]. The peaks in the 2500–2400 cm^{-1}region were associated with asymmetric C–H stretching, symmetric and asymmetric CH_3 vibrations, C stretch, and so forth [5, 7, 25, 31]. This confirmed the presence of HA phase which is in agreement with XRD result.

Fig. 10 shows TEM image of nano HA rod with span 20. It was indicated that the rods had good dispersion with diameter of 15 nm and 80 nm of length. Fig. 11 illustrates the TEM micrograph of nano HA rod with Aliquad as a surfactant

According to the figure, the rods became more agglomerated when the Aliquad was added as a surfactant and there was not a good dispersion (the diameter and length were found to be 20 nm and 100 nm, respectively).

The addition of the surfactants resulted in the formation of an amorphous phase coupled with some hydrates of surfactant. This might be the result of the adsorption of surfactant layer on the surface of the initial HA nuclei, which prevented the aggregation and grain growth of HA in the absence of surfactants that would allow the formation of crystalline phase [10,26,27,32]. However, addition of Aliquad did not play a significant role in the formation of an amorphous HA phase coupled with some hydrates of surfactant, and the most difference observed is in the presence of Span 20 surfactant which is displayed in Fig. 10.

Data suggests that presence of Span 20 was responsible for constrained growth in the directions perpendicular to c axis. Shape control of particles in wet systems was performed by shape controllers adsorbed onto specific surfaces of the particle which reduced the normal growth rate to the adsorbed planes which is in agreement with Gao's research who worked on different surfactants such as CTAB and SDS and found that CTAB as a surfactant had better results [16].

The HA nano rods dried at 100 °C and obtained from both the dialyzed sols were white in color with the powders obtained after dialysis being more free-flowing. Actual removal of adsorbed ions was achieved through repeated change (every 3 h) of the de-ionized water during dialysis. Solution route synthesis of HA nano rods were reported where nano rods were obtained at low temperature.

Fig. 12 shows the XRD pattern of HA nano rod with different time of dialyses. As seen, the main phase in all of patterns was HA, and there was no difference between them

Comparing Fig. 1 (H5) and Fig. 12 (H8) shows the XRD of the HA powders obtained from dialyzed and un-dialyzed sols. Well-developed crystalline

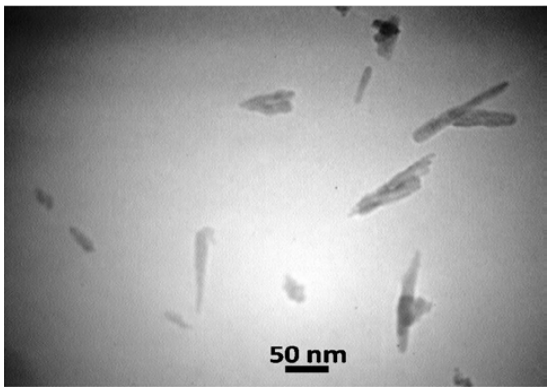

Fig. 10: TEM micrograph of the HA rod in presence of span 20

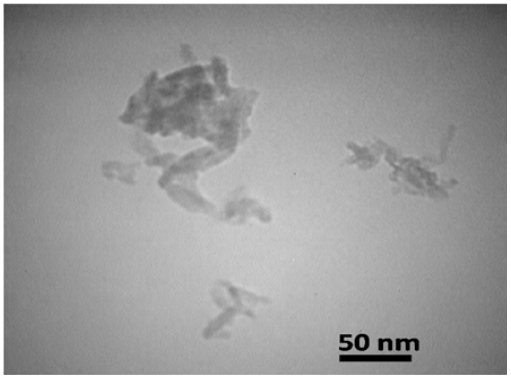

Fig. 11: TEM micrograph of the HA rod in presence of Aliquad

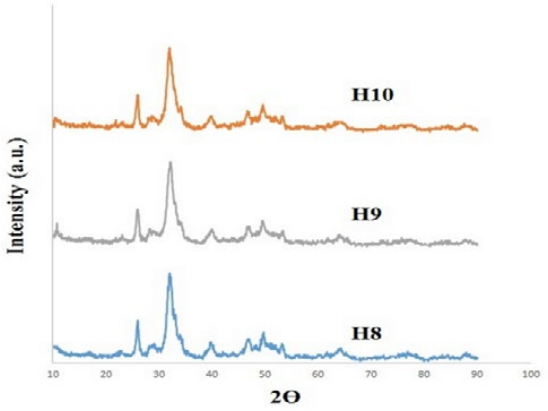

Fig. 12: The XRD pattern of HA nano rod for 12 h of dialyses (H_8) , 15 h of dialyses (H_9) and 18 h of dialyses (H_{10}) after drying at 100 ℃

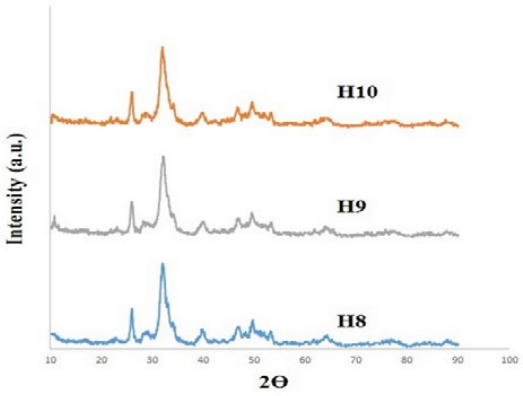

Fig. 13: FTIR curves of HA rod with different dialyses time

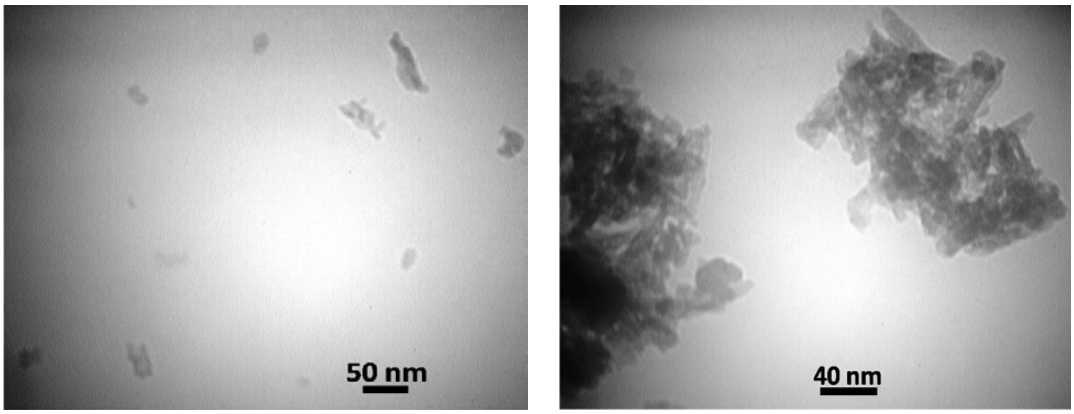

Fig. 14: TEM micrograph of the HA rod a) after 12 h dialyzed, b) after 18 h dialyzed

peaks were noticed in H8 sample with very little background absorption indicating almost complete crystallization rather than H5 sample that may be attributed to the efficient removal of adsorbed ions during dialysis.

The average crystallite size obtained for the nano rods, using Scherrer's equation, was 10 nm for the dialyzed after 12 h and 30 nm for the dialyzed after 15nm h and 40 nm for the dialyzed after 18 h samples. The lower size noticed for the dialyzed samples after 12 h might be attributed to the efficient removal of adsorbed ions during dialysis but the diameter sizes of nano-rods were increased with increasing the dialyzed time which was donated to more water evaporated from sol, caused the supersaturated solution, provided material necessary to bond colliding particles and formed agglomerates.

Fig. 13 shows the FTIR curves of HA rod with different dialyses time. The FTIR spectra demonstrated that the main phase of all three nano rods was mainly HA. However, no significant difference was observed between them. Nonetheless, comparing with Fig. 10, there were some small bonds which were only observed in the un-dialyzed sample showing that the effective removal of the organics was achieved through dialysis. According to Fig. 13, there was not apparent difference between the patterns. As previous patterns, the characteristic signature HA peak near 471,566 and 603 cm^{-1} were attributed to the bending modes of PO_4^{3-} bonds in phosphate groups. [1,28,29]. Moreover, the peaks recognized to phosphate bonds at H_9 and H_{10} were sharper than H_8 which was related to dialysis times [Fig. 13].

Fig. 14 (a,b) show TEM image of HA rods after 12 h dialyzed (a) and after 18 h dialyzed (b). The TEM micrograph of the dialyzed sample after 12 h (Fig. 14 a) shows discrete rod-like HA rods of

uniform size and morphology, having diameter between 10 and 15 nm and length between 50 and 60 nm, indicating elongation along the HA c axis. The systems were performed by shape controllers adsorbed onto specific plan, but the diameters sizes of nano rods were increased with increasing the dialyzed time that provided some agglomeration.

The data suggests that presence of Span 20 and dialyzed time about 12 h were responsible for constrained growth in the directions perpendicular to c axis. This is in agreement with other researchers' results which explored that presence of triethylamine was responsible for constrained growth in the directions perpendicular to c axis (18).

According to Mirjalili [19], agglomeration of solid products from two liquid ionic solutions A and B is as follows: $An^{+} + Bn^{-} \rightarrow C\downarrow$

This reaction involves instantaneous (mixing controlled) chemical reaction, subsequent crystallization of the product (i.e., nucleation and growth of crystals) and its agglomeration.

At low super saturation, there were usually negligible effects of agglomeration, and the crystals size distribution was mainly affected by competition between nucleation and growth of crystal. At high super saturation, the process was dominated by agglomeration. As it preceded more than 12 h, more water evaporated from sol, the supersaturated solution thus supplied material necessary to bond colliding particles and formed agglomerates. Local concentrations also determined electrical interaction between small colloidal particles, because most particles in aqueous media were charged, and resulting repulsion force depended on solution composition [11, 12, 13, 33]. Hence, it would further enhance the agglomeration process for these reasons after 12 h of analyses time which we could see the strongly agglomeration in samples.

CONCLUSION

This study reported synthesis of crystalline HA nanorods of 10 -20 nm diameter and 60-100 nm length using precipitation method**.** The synthesis was done at pH = 10.5-11 condition for 12 h followed by drying at 100 °C**.** The precipitation method was used for the synthesis of nano HA rod which were coupled with the presence of surface active agents, like Span 20 and Aliquad. The results showed that the nano HA rod was obtained at pH of 11 with Span 20 as the surfactant and it had the better effect on dispersion and shape of nano rod than aliquad as a surfactant. The HA nano-rods had an average diameter of 10 nm and length 70-80 nm after 12 h of dialyses time. Selection and control of the precise dialyses time together with surface active agents proved to be important in controlling the rod size, degree of aggregation and the rod shape. It was seen that the separate rod-like HA crystals of uniform size with good dispersion without agglomeration.

CONFLICT OF INTEREST

The authors declare that there is no conflict of interests regarding the publication of this manuscript.

REFERENCES

1. A.I .Misions, T.C.Vaimakis, C.C. Trapalis, Ceram.Inter., 36, 623(2010).
2. C.Ergun, Z. Evis, T.J.Webster, F.C.Sahin , Ceram.Inter., 37, 971(2011).
3. F.N.Okatar, Matter. Let., 60**,** 2207 (2006).
4. F. Deravi , R. Sinatra, O.Christophe, P. Nesmith, H. Yuan, K. Deravi, A. Goss, A. MacQueen, R. Badrossamy, M. Gonzalez, D. Phillips, K. Parker, Mac. Mats. Eng.,1(2017).
5. H.Ji, P. M. Marquis, Bon.Min. Res.,13,744(1992).
6. A.Haider, S. Haider, S.Han ,I.Kang, R. Soc. Chem.,7,7442 (2017).
7. Z.E.Erkmen, Y. Gens , F.N.Oktar, J.A. Ceram. Soc., 90, 2885 (2007).
8. T.Stephanie ,C. Tang, A. Kennedy, S. Talwar,S. A. Khan, J.F.Hydo.,35,36(2014).
9. N.Bahlawane, T.Watanabe, J.A. Ceram. Soc., 9, 2324(2000).
10. Y.Zhao, Y.Qiu, H. Wang, Y.Chen, S. Jin, S. Chen, Inter.J. Poly. Sci.,2016,1(2016).
11. R.T.Franceschi ,B.S. Lyer , Bon. Min. Res.,7, 235(1992).
12. S.Assafi, N.Bruijn, M. Jumaily, W. J. N. Sci. Eng., 6, 58(2016).
13. R.Vaben , D. Stover , J.Mat. Pro. Tech.,92, 84(1999).
14. Y. Lee,S. Fu,C. Lin, 1st Global Conference on Biomedical Engineering & 9th Asian-Pacific Conference on Medical and Biological Engineering, Thailand , pp.9-12(2014).
15. S. Kunjalukkal Padmanabhan , A.Balakrishnan, J.Particulogy,7,466(2009).
16. S. Gao ,K. Sun , A.Li , H.Wang , Maters. Res. Bul, 48, 1003 (2013).
17. S.Tayyebi,F.Mirjalili,H.Samadi,J.Ceram.Pross.17,1034(2016).
18. S. Jadalannagari , S.More, M. Kowshik , S.Ramanan ,Maters .Sci. Eng., 31, 1534 (2011).
19. F. Mirjalili, M. Hasmaliza ,L. Chuah Abdullah, Ceram. Inter. , 36 ,1253(2010).
20. Z. Evis and R. Doremus , Maters. Res. Bul., 43, 2643 (2008).
21. P.Q. Franco, C.F.C. João, B.J.C.Silva , J.P.Borges , Maters.Let., 67, 233(2012).
22. A.Z.Zinchenko , R.H. Davis ,J.Phys. Fluids., 7, 2310(1995).
23. M. Mirjalili,S. Zohoori, J.Nanostruct.Chemis.,6,207(2016).
24. S. Ifuku H. Maeta , H. Izawa, M. Morimoto, H. Saimoto,

RSC. Adv. ,44, 267(2015).
25. M. Maas, P. Guo, M. Keeney, F. Yang, T. M. Hsu, G. Fuller, R. Martin, R. N. Zare, Nano. Lett., 11, 1383(2011).
26. Y. Zhao, Y.Qiu, H.Wang, Y.Chen, S.Jin, S.Chen, Inter. J.Pol. Sci., 2016,17(2016).
27. J. Li, A.He, C. Han, D.Fang, S. Hsiao,B. Chu ,Macro. Molecul. Rap.Com., 27, 114(2006).
28. R.Anamarija, App.Sur. Sci., 296 , 221(2014).
29. W.Cui, Y.Zhou, J Chang, Sci. Technol. Adv. Mater.,11,1(2010).
30. J. Venugopal,S. Low, A.Choon, A. Bharath Kumar, S.Ramakrishna, Art.Org.,32,388(2008).
31. F. Ejaz Ahmed, B. Lalia, R.Hashaikeh, J.Desal., 356 ,15(2015).
32.H.Won,H.Lee,J.Knowless, Bio.M. Res.,79,643(2006).
33.N.Nega,T.Hoai,P.viet, Colls. Sur. B: Bio.Inter.,128,506(2015).